arXiv:1406.7506v1 [physics.optics] 29 Jun 2014

Grating-coupled excitation of the Uller–Zenneck surface wave in the optical regime

Muhammad Faryad and *Akhlesh Lakhtakia*
Nanoengineered Metamaterials Group (NanoMM), Department of Engineering Science and Mechanics, Pennsylvania State University, University Park, PA 16802-6812, USA

Abstract

The excitation of the Uller–Zenneck surface wave in the optical regime was theoretically investigated for planar as well as periodically corrugated interfaces of two homogeneous, isotropic dielectric materials, with only one of the two being dissipative. A practical configuration involving the planewave illumination of a planar interface of the two partnering materials was found to be unsuitable for experimental confirmation of the existence of this surface wave. But, when the interface was periodically corrugated, the Uller–Zenneck wave was found to be excited over a wide range of the angle of incidence. Air and crystalline silicon were identified as suitable partnering materials for experiments in the visible and ultraviolet spectral regimes.

1 Introduction

In 1907, Zenneck published a theoretical analysis of a radio-frequency surface wave guided by the planar interface of air and ground, both assumed homogeneous and isotropic [1]. Subsequently, an electromagnetic surface wave guided by the interface of two homogeneous and isotropic dielectric materials of which only one is dissipative came to be called the Zenneck wave. A 1903 analysis of the same type of wave guided by the interface of a nondissipative dielectric material and (dissipative) seawater by Uller [2] appears to have become obscure, except for citations by both Zenneck [1] and Collin [3]. Since Uller not only obtained but also solved the dispersion equation of the surface wave, albeit under the special conditions of seawater being significantly conductive and the (real) relative permittivity of seawater being much larger than that of its partnering material (air?), we think it is appropriate to name this surface wave after both Uller and Zenneck.

Sommerfeld [4, 5] provided a rigorous mathematical analysis of the Uller–Zenneck wave; see also a review by Wait [6]. As the ground is not metallic but is a dissipative dielectric material, the Uller–Zenneck wave must be distinguished from the surface plasmon-polariton (SPP) wave that is usually taken to be guided by the interface of a lossless dielectric material and a metal, both assumed homogeneous and isotropic [7, 8].

Although sometimes ignored [9, 10], the distinction between SPP and Uller–Zenneck waves has a significant consequence. Unlike an SPP wave, whose phase speed is smaller than that of a plane wave in the partnering dielectric material, the phase speed of an Uller–Zenneck wave is usually larger than the phase speeds of plane waves in both partnering dielectric materials. Accordingly, unlike the SPP wave [8], the Uller–Zenneck wave can be

excited without the use of a coupling prism or a surface-relief grating. All that is needed is to illuminate the guiding planar interface by a highly obliquely incident plane wave.

But, that very same characteristic leads to difficulties in distinguishing the Uller–Zenneck wave from other waves in the radio-frequency regime [6]. Experimental observation of the Uller–Zenneck wave in the same spectral regime [11] remains mired in confusion [12]. Part of the reason for confusion about the Uller–Zenneck wave is an infelicitous connection with the Brewster phenomenon [13, 3].

Theory, on the other hand, is unequivocal. Uller [2], Zenneck [1], and Sommerfeld [4, 5] had investigated the canonical boundary-value problem depicted schematically in Fig. 1(a). In this figure, the nondissipative dielectric partnering material with relative permittivity ε_d ($\mathrm{Re}(\varepsilon_d) > 0$, $\mathrm{Im}(\varepsilon_d) = 0$) occupies the half space $z < 0$; the dissipative dielectric partnering material with relative permittivity ε_s ($\mathrm{Re}(\varepsilon_s) > 0$, $\mathrm{Im}(\varepsilon_s) > 0$) occupies the half space $z > 0$; and the Uller–Zenneck wave propagates parallel to the x axis, decays as $|z| \to \infty$, and does not depend on y. The wave has to be p polarized (i.e., $\hat{\mathbf{u}}_y \cdot \mathbf{E} = 0$ and $\hat{\mathbf{u}}_x \cdot \mathbf{H} = \hat{\mathbf{u}}_z \cdot \mathbf{H} = 0$, where the Cartesian unit vectors are identified as $\hat{\mathbf{u}}_x$, $\hat{\mathbf{u}}_y$, and $\hat{\mathbf{u}}_z$). The dispersion equation is readily solvable [14].

However, the canonical boundary-value problem is not implementable practically. At the very least, the dissipative partnering material has to have a large but finite thickness L_m, as shown schematically in Fig. 1(b), and a p-polarized plane wave has to be incident on the interface $z = 0$ from the half space $z < 0$. Instead of a p-polarized plane wave, an angular spectrum of p-polarized plane waves emanating from a finite source can be used [15, 16]. Air has been taken as the nondissipative partnering material in most radio-frequency experiments [11]. But the evidence for the excitation of the Uller–Zenneck wave in this configuration is ambiguous [12, 6].

The grating-coupled configuration [17] provides an alternative. As shown in Fig. 1(c), the interface of the two partnering materials is periodically corrugated in this configuration. Although some evidence is available from a finite-element simulation [18] in the radio-frequency regime, with the periodic corrugations modeled as an impedance plane with periodically varying surface impedance, no comparison was made in that study against the underlying canonical boundary-value problem and the localization of the surface wave was not explicitly demonstrated.

Since the grating-coupled configuration is practicable in the optical regime [8, 19], we decided to examine theoretically if unambiguous experimental evidence of the Uller–Zenneck wave can be obtained therefrom. Therefore, the grating-coupled configuration is the focus of this paper, although the underlying canonical boundary-value problem and excitation using the planar interface were also investigated.

The plan of this paper is as follows: The canonical boundary-value problem is briefly discussed and numerical results are presented in Sec. 2. Excitation of the Uller–Zenneck wave by a plane wave obliquely incident at the interface $z = 0$, when the dissipative partnering material has a large but finite thickness, is discussed in Sec. 3. The numerical

results for the grating-coupled configuration are discussed in Sec. 4. Concluding remarks are presented in Sec. 5. An $\exp(-i\omega t)$ dependence on time t is implicit, with ω denoting the angular frequency and $i = \sqrt{-1}$. Vectors are in boldface. The free-space wavenumber and wavelength are denoted by $k_0 = \omega\sqrt{\varepsilon_0\mu_0}$ and $\lambda_0 = 2\pi/k_0$, respectively, with μ_0 and ε_0 being the permeability and permittivity of free space, respectively.

2 Canonical boundary-value problem

Let us begin with the canonical boundary-value problem, shown schematically in Fig. 1(a). The surface wave has to be p polarized. If it is taken to propagate parallel to the x axis in the xz plane, the electric field phasors in the two contiguous half spaces may be written as

$$\mathbf{E}(\mathbf{r}) = a_p \left(\frac{\alpha_d \hat{\mathbf{u}}_x + q\hat{\mathbf{u}}_z}{k_0 n_d} \right) \exp\left[i\left(qx - \alpha_d z \right) \right] , \quad z < 0 \, , \tag{1}$$

and

$$\mathbf{E}(\mathbf{r}) = b_p \left(\frac{-\alpha_s \hat{\mathbf{u}}_x + q\hat{\mathbf{u}}_z}{k_0 n_s} \right) \exp\left[i\left(qx + \alpha_s z \right) \right] , \quad z > 0 \, , \tag{2}$$

where $n_d = \sqrt{\varepsilon_d} > 0$, $n_s = \sqrt{\varepsilon_s}$, $q^2 + \alpha_s^2 = k_0^2\,\varepsilon_s$, and $q^2 + \alpha_d^2 = k_0^2 \varepsilon_d$. Furthermore, q is complex valued, $\mathrm{Im}(\alpha_d) > 0$ for attenuation as $z \to -\infty$, and $\mathrm{Im}(\alpha_s) > 0$ for attenuation as $z \to \infty$. Finally a_p and b_p are unknown scalars with the same units as the electric field.

The dispersion equation of the Uller–Zenneck wave can be found after enforcing the standard boundary conditions at the interface $z = 0$. The solution of the dispersion equation is

$$q = k_0 \sqrt{\frac{\varepsilon_d \varepsilon_s}{\varepsilon_d + \varepsilon_s}} \, , \tag{3}$$

where

$$\alpha_d = k_0 \frac{\varepsilon_d}{\sqrt{\varepsilon_d + \varepsilon_s}} \, , \quad \alpha_s = k_0 \frac{\varepsilon_s}{\sqrt{\varepsilon_d + \varepsilon_s}} \, . \tag{4}$$

For illustrative numerical results throughout this paper, we identified crystalline silicon as the dissipative partnering material and air as the nondissipative partnering material. The relative permittivity ε_s of crystalline silicon is presented in Fig. 2 as a function of λ_0 [20], whereas ε_d was taken to be unity.

Figure 3(a) presents the spectrum of $\mathrm{Re}(q)/k_0 n_d$ for $\lambda_0 \in [250, 600]$ nm. As silicon is metallic for $\lambda_0 \leq 293$ nm because $\mathrm{Re}(\varepsilon_s) < 0$, the surface wave must be classified as an SPP wave. However, silicon is a dielectric material, though very dissipative, for $\lambda_0 \geq 294$ nm because $\mathrm{Re}(\varepsilon_s) > 0$; hence, the surface wave must then be classified as an Uller–Zenneck wave. Let us also note that $\mathrm{Re}(q) > k_0 n_d$ for SPP waves and $\mathrm{Re}(q) \lesssim k_0 n_d$ for Uller–Zenneck waves.

The propagation length $\Delta_{prop} = 1/\mathrm{Im}\,(q)$ is presented in Fig. 3(b) as a function of λ_0. Whereas $\Delta_{prop} < 5$ μm for the SPP wave, the propagation length of the Uller–Zenneck wave lies between 5 and 700 μm. In general, Δ_{prop} increases as λ_0 increases since $\mathrm{Im}(\varepsilon_s)$ decreases. The increase of the propagation length is also accompanied by increases in the penetration depth $\Delta_d = 1/\mathrm{Im}\,(\alpha_d)$ of the surface wave in the nondissipative partnering material and the penetration depth $\Delta_s = 1/\mathrm{Im}\,(\alpha_s)$ into the dissipative partnering material, as also shown in Fig. 3(b).

Although the canonical problem is not practically implementable, predictions of $\mathrm{Re}(q)$ provided by its solution are valuable in designing practical configurations. With air as the nondissipative partnering material, two practical configurations are considered next. In both configurations, the dissipative partnering material is present as a slab of finite thickness. A p-polarized plane wave is obliquely incident on one face of this slab. The face can be either planar (Sec. 3) or periodically corrugated (Sec. 4).

3 Practical configuration with planar guiding interface

As shown in Fig. 1(b), let the half spaces $z < 0$ and $z > L_m$ be filled with a homogeneous material of relative permittivity ε_d, while the region $0 < z < L_m$ is occupied by a homogeneous material of relative permittivity ε_s. A p-polarized plane wave is obliquely incident on the plane $z = 0$, its wave vector making an angle θ with respect to the z axis. Equation (3) predicts that a surface wave will be excited when $\theta = \theta^{\mathrm{C}} = \sin^{-1}\left[\mathrm{Re}(q)/k_0 n_d\right]$.

The electric field phasor in the half space $z < 0$ is given by

$$\begin{aligned}\mathbf{E}(\mathbf{r}) &= \left(-\hat{\mathbf{u}}_x \cos\theta + \hat{\mathbf{u}}_z \sin\theta\right) \exp\left[ik_0 n_d \left(x\sin\theta + z\cos\theta\right)\right] \\ &\quad + r_p \left(\hat{\mathbf{u}}_x \cos\theta + \hat{\mathbf{u}}_z \sin\theta\right) \exp\left[ik_0 n_d \left(x\sin\theta - z\cos\theta\right)\right] , \quad z < 0 , \end{aligned} \tag{5}$$

where r_p is the reflection coefficient. In the half space $z > L_m$, the electric field phasor is given by

$$\mathbf{E}(\mathbf{r}) = t_p \left(-\hat{\mathbf{u}}_x \cos\theta + \hat{\mathbf{u}}_z \sin\theta\right) \exp\left\{ik_0 n_d \left[x\sin\theta + (z - L_m)\cos\theta\right]\right\} , \quad z > L_m, \tag{6}$$

where t_p is the transmission coefficient. The reflectance $R_p = |r_p|^2$, the transmittance $T_p = |t_p|^2$, and the absorptance $A_p = 1 - (R_p + T_p)$ can be computed as functions of λ_0 and θ for any value of L_m using a textbook procedure [21].

The plot of θ^{C} as a function of λ_0 for air and crystalline silicon as the partnering materials is presented in Fig. 4(a). For $L_m = 250$ nm, A_p, R_p, and T_p as functions of λ_0 and θ are presented in Figs. 4(b), (c), and (d), respectively. No sharp absorptance band—that could signify the excitation of a surface wave [22]—is present in Fig. 4(b). Neither

are any similar signatures of the excitation of surfaces waves present in Figs. 4(c) and (d). The same conclusions were drawn for other values of $L_m \in [100, 1000]$ nm.

Parenthetically, the wide absorptance band in Fig. 4(b) delineated approximately by $\lambda_0 \in [275, 425]$ nm and $\theta \in [60^\circ, 85^\circ]$ does not indicate surface-wave excitation. For any fixed value of λ_0, the center of the θ-range of this band is significantly different from θ^{C}. Moreover, the θ-range is far too broad to signify the excitation of any surface wave.

This practical configuration is the one employed for most experimental investigations of the Uller–Zenneck wave. Figure 4 leads to the conclusion that this configuration is not appropriate to unambiguously confirm the existence of the Uller–Zenneck wave.

4 Practical configuration with periodically corrugated guiding interface

Let us now consider the excitation of the Uller–Zenneck wave in the grating-coupled configuration, shown schematically in Fig. 1(c). The regions $z < 0$ and $z > L_t = L_g + L_m$ are occupied by a homogeneous material of relative permittivity ε_d, the region $L_g < z < L_t$ is occupied by a homogeneous material of relative permittivity ε_s, and the region $0 < z < L_g$ contains a rectangular grating of period L along the x axis and duty cycle $\zeta \in (0, 1)$. Let a p-polarized plane wave be obliquely incident upon the grating. The wave vector of the incident plane wave lies wholly in the xz plane and is oriented at an angle θ with respect to the z axis.

The electric field phasor in the half space $z < 0$ is adequately represented by [17, 14]

$$\begin{aligned} \mathbf{E}(\mathbf{r}) &= (-\hat{\mathbf{u}}_x \cos\theta + \hat{\mathbf{u}}_z \sin\theta) \exp\left[ik_0 n_d \left(x \sin\theta + z \cos\theta\right)\right] \\ &\quad + \sum_{n=-N_t}^{N_t} r_p^{(n)} \mathbf{p}_n^- \exp\left[i\left(\kappa^{(n)} x - \alpha^{(n)} z\right)\right], \quad z \le 0\,. \end{aligned} \tag{7}$$

Here, $N_t > 0$ is a sufficiently large integer, $r_p^{(n)}$ is the amplitude of the Floquet harmonic of order $n \in \{0, \pm 1, \pm 2, ..., \pm N_t\}$ in the reflected field, with

$$\kappa^{(n)} = k_0 n_d \sin\theta + 2\pi n / L\,, \tag{8}$$

$$\alpha^{(n)} = \begin{cases} +\sqrt{k_0^2 \varepsilon_d - \left(\kappa^{(n)}\right)^2}\,, & k_0^2 \varepsilon_d \ge \left(\kappa^{(n)}\right)^2 \\ +i\sqrt{\left(\kappa^{(n)}\right)^2 - k_0^2 \varepsilon_d}\,, & k_0^2 \varepsilon_d < \left(\kappa^{(n)}\right)^2 \end{cases}, \tag{9}$$

$$\mathbf{p}_n^{\pm} = \frac{\mp \alpha^{(n)} \hat{\mathbf{u}}_x + \kappa^{(n)} \hat{\mathbf{u}}_z}{k_0 n_d}\,. \tag{10}$$

In the half space $z > L_t$, the electric field phasor is given by

$$\mathbf{E}(\mathbf{r}) = \sum_{n=-N_t}^{N_t} t_p^{(n)} \mathbf{p}_n^+ \exp\left\{ i \left[\kappa^{(n)} x + \alpha^{(n)} \left(z - L_t \right) \right] \right\} , \quad z > L_t \, , \tag{11}$$

where $t_p^{(n)}$ is the amplitude of the Floquet harmonic of order n in the transmitted field. Whereas $n = 0$ identifies the specular components of the reflected and transmitted fields, the non-specular components are identified by $n \neq 0$.

The reflectances and transmittances of order n are defined as

$$R_p^{(n)} = |r_p^{(n)}|^2 \, \frac{\mathrm{Re}\left(\alpha^{(n)}\right)}{\alpha^{(0)}} \, , \quad T_p^{(n)} = |t_p^{(n)}|^2 \, \frac{\mathrm{Re}\left(\alpha^{(n)}\right)}{\alpha^{(0)}} \, , \tag{12}$$

respectively; the total reflectance and the total transmittance as

$$R_p = \sum_{n=-N_t}^{N_t} R_p^{(n)} \, , \quad T_p = \sum_{n=-N_t}^{N_t} T_p^{(n)} \, , \tag{13}$$

respectively; and the absorptance as

$$A_p = 1 - \left(R_p + T_p \right) . \tag{14}$$

The rigorous coupled-wave approach [17, 23, 24, 14] was used to compute the reflection and transmission amplitudes. As for the previous two sections, air was chosen as the nondissipative partnering material and crystalline silicon as the dissipative partnering material. All calculations were made for $L_g = 35$ nm, $L = 350$ nm, $\zeta = 0.5$, and $L_m = 1000$ nm. We set $N_t = 13$ after ascertaining that absorptance converged within a preset tolerance of $\pm 1\%$.

According to Eq. (3), an Uller–Zenneck wave could be excited when θ equals

$$\theta_n^{\mathrm{C}} = \sin^{-1} \left\{ \frac{\mathrm{Re}(q) - 2\pi n / L}{k_0 n_d} \right\} \tag{15}$$

for some $n \in \mathbb{Z}$. Values of θ_n^{C} for $n \in \{-2, -1, 0, 1\}$ are plotted in Fig. 5(a) as functions of λ_0. The absorptance A_p, the specular reflectance $R_p^{(0)}$, and total transmittance T_p as functions of λ_0 and θ are presented in Figs. 5(b), (c), and (d), respectively. The plot of A_p in Fig. 5(b) clearly shows the presence of sharp absorptance bands corresponding to θ_n^{C} for $n = \pm 1$ in Fig. 5(a) predicted by the canonical boundary-value problem. A somewhat less sharp absorptance band for $n = -2$ also exists. These absorptance bands are independent of the thickness $L_m > 2\lambda_0$ and indicate the excitation of the Uller–Zenneck wave.

A wide absorptance band in Fig. 5(b) delineated approximately by $\lambda_0 \in [375, 525]$ nm and $\theta \in [50^\circ, 80^\circ]$ does not represent the excitation of the Uller–Zenneck wave because, for

any fixed value of λ_0, the center of the θ-range of this band is significantly different from θ_0^{C} in Fig. 5(a). Moreover, the θ-range is far too broad to signify the excitation of any surface wave.

Let us recall from Sec. 2 that the surface wave guided by the planar interface of air and silicon is an SPP wave for $\lambda_0 \leq 293$ nm and an Uller–Zenneck wave for $\lambda_0 \geq 294$ nm. A scan of Figs. 5(a), (b), and (c) suggests that the SPP wave blends into the Uller–Zenneck wave as λ_0 increases, there being no discernible difference between the pertinent absorptance bands across $\lambda_0 \sim 293.5$ nm.

The plot of the specular reflectance $R_p^{(0)}$ in Fig. 5(c) shows the signatures of the absorptance bands representing the excitation of the Uller–Zenneck wave for $n = \pm 1$ in Fig. 5(b). Since the specular reflectance is not difficult to measure for $\theta \gtrsim 10^\circ$, the grating-coupled configuration appears to be very appropriate for experimental confirmation of the existence of the Uller–Zenneck wave. The selected combination of partnering materials—viz., air and silicon—is suitable because Fig. 5(d) indicates that the total transmittance is very low in the chosen spectral regime due to the high absorption of light in silicon.

5 Concluding remarks

We investigated theoretically the excitation of the Uller–Zenneck wave guided by the interface of two homogeneous and isotropic dielectric materials, of which only one is dissipative. Although the solution of the canonical boundary-value problem—involving the propagation of the Uller–Zenneck wave guided by the interface of two contiguous half spaces occupied by the two partnering materials—clearly indicates the possibility of surface-wave propagation, a practical configuration involving the planewave illumination of a planar interface did not offer any corroborating evidence. It is therefore not surprising that this configuration, although often used in the past for experimental investigations of the Uller–Zenneck wave, has not yielded unambiguous confirmation of the existence of this type of surface wave.

In contrast, another practical configuration involving the planewave illumination of a periodically corrugated interface of the two partnering materials was shown by us to offer unambiguous confirmation of the existence of the Uller–Zenneck wave. This surface wave can be excited as a Floquet harmonic of order $n \neq 0$ for a wide range of the angle of incidence in the grating-coupled configuration.

We hope that this paper will set the stage for the first conclusive experimental evidence of the existence of the Uller–Zenneck wave. Such a development will be helpful in broadening the horizons of the applications of surface waves due to the availability of more choices of partnering materials.

Acknowledgements. The authors thank the US National Science Foundation for partial financial support via grant DMR-1125590. AL also thanks the Charles Godfrey Binder

Endowment at the Pennsylvania State University for ongoing support of his research activities.

References

[1] J. Zenneck, "Über die Fortpflanzung ebener elektromagnetischer Wellen längs einer ebenen Lieterfläche und ihre Beziehung zur drahtlosen Telegraphie," *Ann. Phys. Lpz.* **23**, 846–866 (1907).

[2] K. Uller, *Beiträge zur Theorie der Elektromagnetischen Strahlung* (Ph.D. Thesis, Universität Rostock, Germany, 1903); Chapter XIV.

[3] R. E. Collin, *Field Theory of Guided Waves, 2nd ed.* (Wiley, 1991).

[4] A. Sommerfeld, "Über die Ausbreitung der Wellen in der drahtlosen Telegraphie," Ann. Phys. Lpz. **28**, 665–736 (1909).

[5] A. Sommerfeld, "Über die Ausbreitung der Wellen in der drahtlosen Telegraphie," Ann. Phys. Lpz. **81**, 1135–1153 (1926).

[6] J. R. Wait, "The ancient and modern history of EM ground-wave propagation," IEEE Antennas Propagat. Mag. **40**(5), 7–24 (1998), October issue.

[7] S. A. Maier, *Plasmonics: Fundamentals and Applications* (Springer, 2007).

[8] J. Homola (ed.), *Surface Plasmon Resonance Based Sensors* (Springer, 2006).

[9] T.-I. Jeon and D. Grischkowsky, "THz Zenneck surface wave (THz surface plasmon) propagation on a metal sheet," Appl. Phys. Lett. **88**, 061113 (2006).

[10] M. Navarro-Cía, M. Natrella, F. Dominec, J. C. Delagnes, P. Kužel, P. Mounaix, C. Graham, C. C. Renaud, A. J. Seeds, and O. Mitrofanov, "Terahertz imaging of sub-wavelength particles with Zenneck surface waves," Appl. Phys. Lett. **103**, 221103 (2013).

[11] V. I. Baĭbakov, V. N. Datsko, and Yu. V. Kistovich, "Experimental discovery of Zenneck's surface electromagnetic waves," Sov. Phys. Usp. **32**, 378–379 (1989).

[12] V. N. Datsko and A. A. Kopylov, "On surface electromagnetic waves," Sov. Phys. Usp. **51**, 101–102 (2008).

[13] J. R. Wait, *Electromagnetic Waves in Stratified Media, 2nd ed.* (Pergamon, 1970).

[14] J. A. Polo Jr., T. G. Mackay, and A. Lakhtakia, *Electromagnetic Surface Waves: A Modern Perspective* (Elsevier, 2013).

[15] D. A. Hill and J. R. Wait, "Excitation of the Zenneck surface wave by a vertical aperture," Radio Sci. **13**, 969–977 (1978).

[16] D. A. Hill and J. R. Wait, "On the excitation of the Zenneck surface wave over the ground at 10 MHz," Ann. Télécommun. **35**, 179–182 (1980).

[17] M. Faryad and A. Lakhtakia, "Grating-coupled excitation of multiple surface plasmon-polariton waves," Phys. Rev. A **84**, 033852 (2011).

[18] J. Hendry, "Isolation of the Zenneck surface wave," 2010 Loughborough Antenas & Propagation Conference, Loughborough, UK, 8–9 November (2010).

[19] D. P. Pulsifer, M. Faryad, A. Lakhtakia, A. S. Hall, and L. Liu, "Experimental excitation of the Dyakonov–Tamm wave in the grating-coupled configuration," Opt. Lett. **39**, 2125–2128 (2014).

[20] Data on relative permittivity of crystalline silicon as a function of λ_0 were downloaded from http://refractiveindex.info/legacy/?group=CRYSTALS&material=Si&option=Palik&wavelength=6.1 on 1 May 2014.

[21] M. Born and E. Wolf, *Principles of Optics, 7th ed.* (Pergamon, 1999).

[22] A. S. Hall, M. Faryad, G. D. Barber, L. Liu, S. Erten, T. S. Mayer, A. Lakhtakia, and T. E. Mallouk, "Broadband light absorption with multiple surface plasmon polariton waves excited at the interface of a metallic grating and photonic crystal," ACS Nano **7**, 4995–5007 (2013).

[23] L. Li, "Multilayer modal method for diffraction gratings of arbitrary profile, depth, and permittivity," J. Opt. Soc. Am. A **12**, 2581–2591 (1993).

[24] M. G. Moharam, E. B. Grann, and D. A. Pommet, "Formulation for stable and efficient implementation of the rigorous coupled-wave analysis of binary gratings," J. Opt. Soc. Am. A **12**, 1068–1076 (1995).

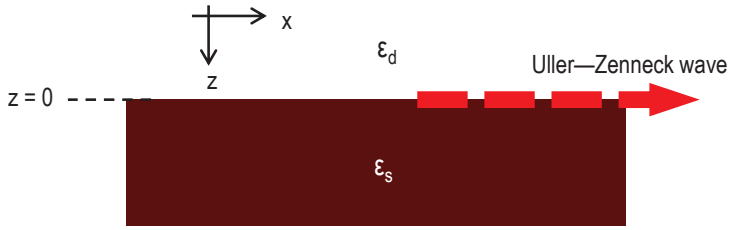

(a) Canonical boundary-value problem

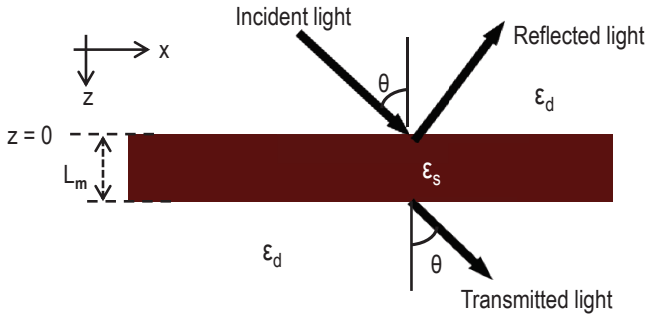

(b) Practical configuration with planar guiding interface

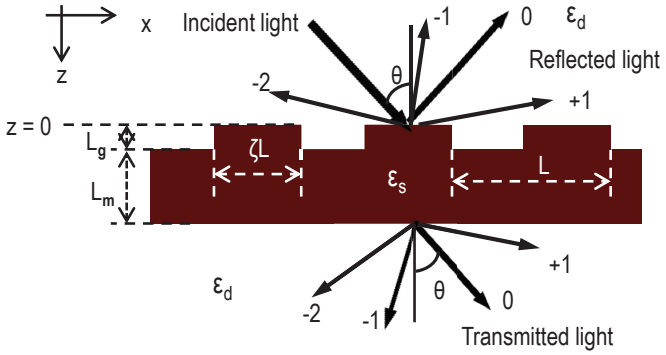

(c) Practical configuration with periodically corrugated guiding interface

Figure 1: (a) Schematic of the canonical boundary-value problem. The Uller–Zenneck wave is guided by the interface $z = 0$. (b) Excitation of the Uller–Zenneck wave by a plane wave that is obliquely incident at the interface $z = 0$, when the dissipative partnering material has a large but finite thickness. (c) Schematic of the grating-coupled configuration. Same as (b), but the guiding interface is periodically corrugated. The specular components of the reflected and transmitted fields are labeled as 0, whereas their non-specular components are labeled by non-zero integers.

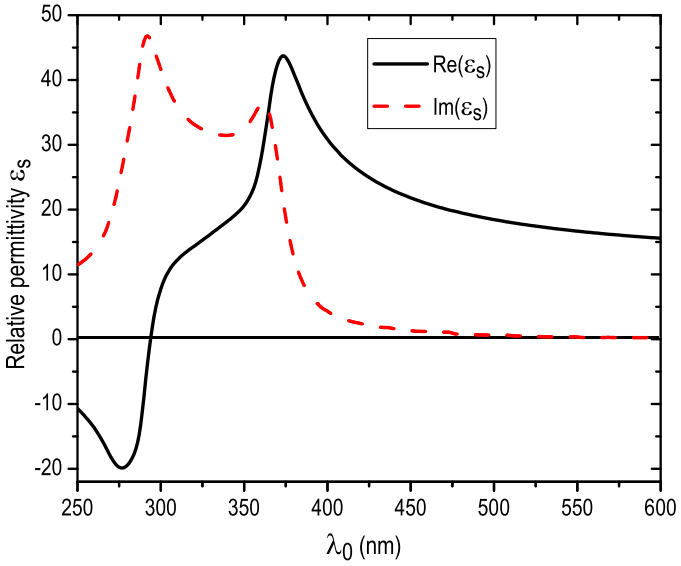

Figure 2: Real and imaginary parts of the relative permittivity ε_s of crystalline silicon as functions of λ_0 [20].

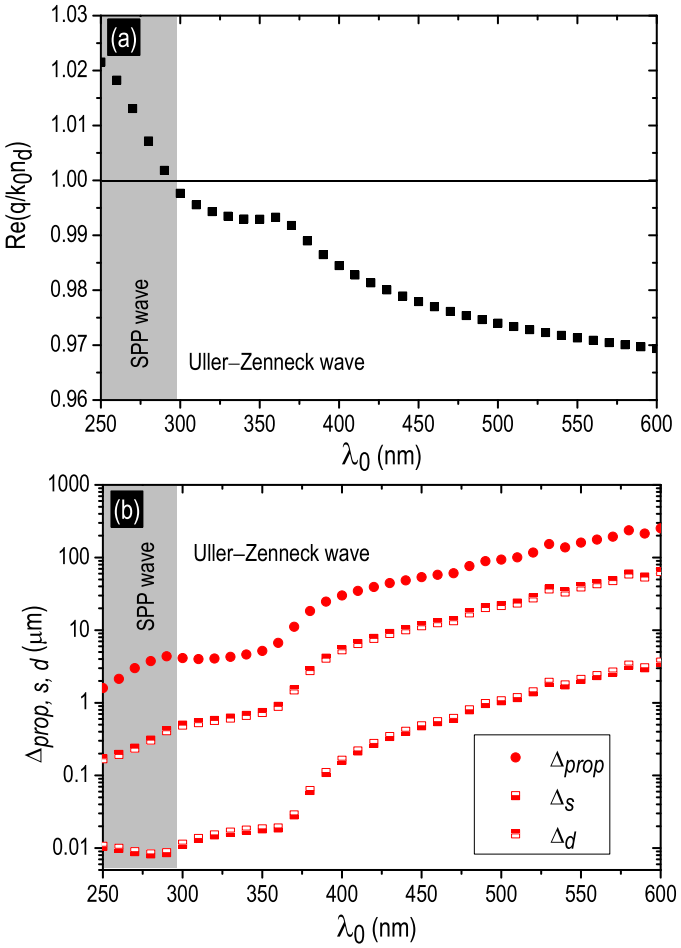

Figure 3: Canonical boundary-value problem. (a) Spectrum of $\mathrm{Re}(q)/k_0 n_d$ for the surface wave guided by the planar interface of air and crystalline silicon. (b) Spectrums of Δ_{prop}, Δ_d, and Δ_s. The surface wave is an SPP wave for $\lambda_0 < 293$ nm and an Uller–Zenneck wave for $\lambda_0 \geq 294$ nm.

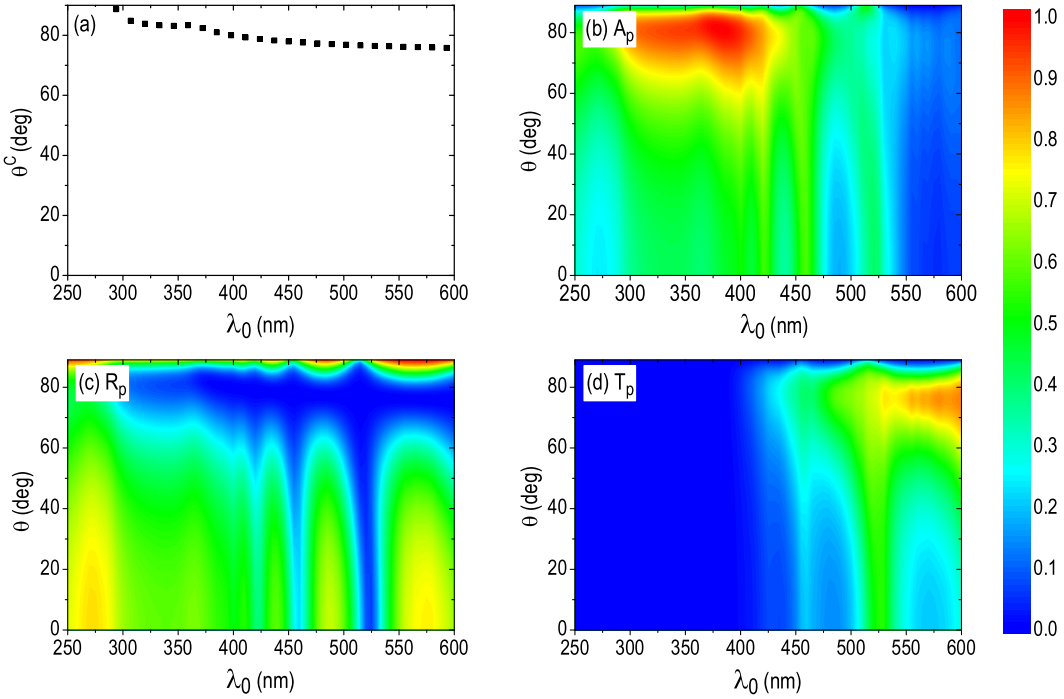

Figure 4: Practical configuration with planar guiding interface. (a) Spectrum of $\theta^{\mathrm{C}} = \sin^{-1}[\mathrm{Re}(q)/k_0 n_d]$ when the excitation of the Uller–Zenneck wave is predicted by the solution of the canonical boundary-value problem. (b) Absorptance A_p, (c) reflectance R_p, and (d) transmittance T_p as functions of λ_0 and θ when $L_m = 250$ nm.

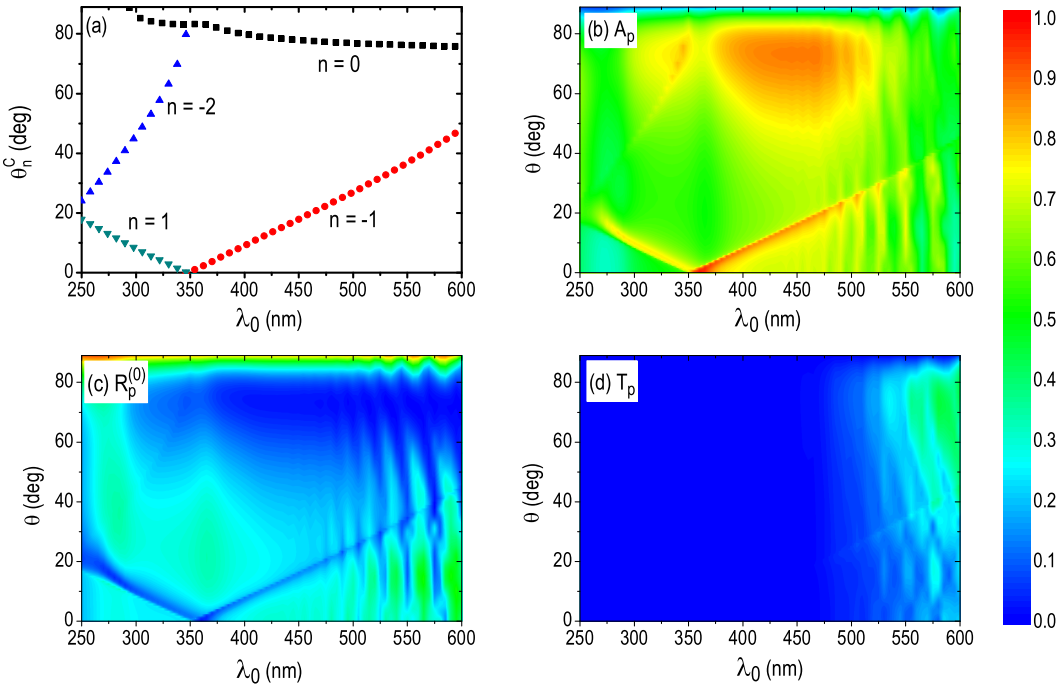

Figure 5: Practical configuration with periodically corrugated guiding interface. (a) Spectrums of $\theta_n^{\mathrm{C}} = \sin^{-1}\{[\mathrm{Re}(q) - 2\pi n/L]/k_0 n_d\}$ when the excitation of the Uller–Zenneck wave is predicted by the solution of the canonical boundary-value problem. (b) Absorptance A_p, (c) specular reflectance $R_p^{(0)}$, and (d) total transmittance T_p as functions of λ_0 and θ when $L = 350$ nm, $L_g = 35$ nm, $\zeta = 0.5$, and $L_m = 1000$ nm.